Proceedings of ISFOG 2025
5TH INTERNATIONAL SYMPOSIUM ON
FRONTIERS IN OFFSHORE GEOTECHNICS
Nantes, France | June 9-13 2025

ISBN 978-2-85782-758-0

Helically embedded plate anchors for floating offshore wind: potential and proof of concept

W. Hidayat*
Centre for Offshore Foundation Systems, The University of Western Australia, Perth, Australia

J.A. Nietiedt, C.D. O'Loughlin, P.G. Watson, C. Gaudin
Centre for Offshore Foundation Systems, The University of Western Australia, Perth, Australia

D. Bertalot, M.J. Rattley, S.A. Whyte
Geowynd, London, United Kingdom

M. Brown
University of Dundee, Dundee, United Kingdom

**wirman.hidayat@research.uwa.edu.au (corresponding author)*

ABSTRACT: Helical anchors are a promising solution for anchoring floating offshore wind turbines, offering high holding capacity relative to their dry weight and noiseless installation. However, practical challenges associated with potentially high torque requirements coupled with their relatively poor performance under lateral loading have hampered their uptake by the offshore industry. This paper introduces the Helically Embedded PLate Anchor (HEPLA), a new anchor concept that is installed as a screw pile but loaded as a plate anchor. Installation involves rotating and pushing the follower shaft to reach a target depth, after which the shaft is detached and retrieved for subsequent installations, leaving only the helical plate embedded in the seabed. Proof-of-concept experiments conducted in a geotechnical centrifuge in overconsolidated kaolin clay show that the HEPLA concept is feasible, practical, and results in behaviour that is consistent with conventional helical anchors. The results indicate that the HEPLA has the potential to be a cost-effective and viable alternative offshore anchoring system, requiring lower installation torque than a conventional helical anchor (as the shaft can be smaller), less overall steel as the follower shaft is reused across installations, and significant resistance under non-vertical loading.

Keywords: centrifuge modelling, embedded mooring chain, helical anchors, plate anchors

1 INTRODUCTION

Floating offshore wind is a promising renewable energy technology that allows strong wind resources to be exploited in deep offshore waters where fixed-bottom turbines are not technically or economically feasible. To support this development, a reliable and economical anchoring system is needed to secure the floating wind turbines to the seabed. Helical anchors have been proposed as a potential solution (Byrne & Houlsby, 2015), providing a high capacity as a ratio of their dry weight. Furthermore, installation of helical anchors is silent, thereby causing minimal disturbance to marine life compared to pile-driving (Bailey et al., 2010).

Despite this potential and being widely used onshore, helical anchors face practical challenges for offshore use. The large environmental offshore loads necessitate scaling up the size of the helical anchor, resulting in increased installation torque and thrust force, which exceeds the capacity of currently available equipment (Davidson et al., 2022). Recent work conducted in both sand (Cerfontaine et al., 2023; Duverneuil, 2024) and clay (Ullah et al., 2024) has shown that the thrust force issue can be mitigated by lowering the advancement ratio (*AR*, defined as the vertical displacement per rotation divided by the helix pitch). However, controlling *AR* may be impractical in the field, as it could necessitate a significant installation force. Instead, installing the anchor with a constant thrust force – simulating the anchor weight plus any additional ballast that may be required – is likely to be a more practical installation technique. Catenary and taut/semi-taut mooring configurations require resistance to large horizontal load components, which presents a significant challenge for helical anchors given the relatively small shaft diameter compared to conventional pile foundations (Al-Baghdadi et al., 2015).

This paper introduces the Helically Embedded PLate Anchor (HEPLA), a new anchor concept that is installed in an identical way as a conventional helical anchor but has a removable follower shaft such that when the helical plate reaches the targeted embedment depth, the follower shaft can be removed and reused for subsequent installations, leaving the helical plate (and an attached mooring) in the seabed, such that it acts as a plate anchor (as shown in Figure 1). The HEPLA combines the efficient pull-out capacity of the helical anchor with the cost-effectiveness of using a smaller and reusable shaft. The solution maintains the main benefits of helical anchors whilst also providing a feasible solution for sustaining high lateral load components, as the helical plate will reorientate itself to the direction of the load. The HEPLA concept leverages ideas from other 'hybrid' anchoring systems, such as the Suction Embedded PLate Anchor (SEPLA) (Dove et al., 1998) and Dynamically Embedded PLate Anchor (DEPLA) (O'Loughlin et al., 2013) – with both of these systems utilising direct embedment techniques that incorporate a follower to install a plate anchor.

This paper describes experiments conducted in a geotechnical centrifuge that form the proof of concept for HEPLAs. These experiments were conducted in an overconsolidated clay and are part of a broader, ongoing experimental program that considers a range of coarse- and fine-grained soils.

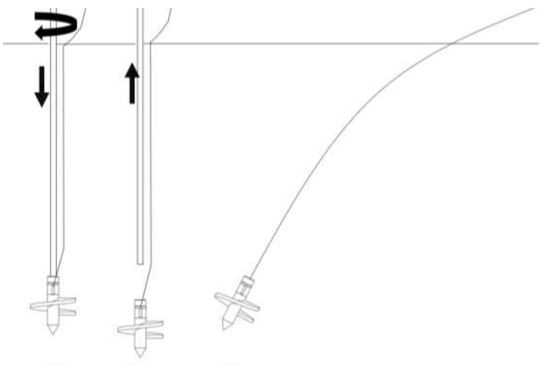

Figure 1. HEPLA concept: (a) installation by rotating and pushing the shaft; (b) shaft retrieval and reuse; (c) tensioning on the mooring line.

2 METHODOLOGY

2.1 Centrifuge modelling and soil properties

The experiments were performed using the 3.6 m diameter beam centrifuge at the National Geotechnical Centrifuge Facility (NGCF) at the University of Western Australia (UWA). A clay slurry was prepared by mixing kaolin clay powder with water at a water content of 120% in a mechanical mixer under vacuum for 24 hours. This slurry was then poured into a sample container ('strongbox') measuring 650 mm in length, 390 mm in width and 325 mm in height, with a drainage layer of sand overlain by a sheet of geofabric at the base of the strongbox providing base drainage. Drainage pipes in the corners of the sample connected this drainage layer to the free water on top of the sample, providing two-way drainage. A pore pressure transducer was placed approximately at the mid-height of the sample to assess the degree of consolidation of the sample at the longest drainage path. The clay was consolidated in a press on the laboratory floor to a maximum stress of 400 kPa, achieving a final sample height of 220 mm. The sample was then transferred to the centrifuge where it was spun for a further 24 hours at the testing acceleration of 80*g* before commencing the tests. This resulted in an OCR of 5.5 at the target helix depth of 150 mm (H/D = 6). The properties of the kaolin clay used in this study are summarised in Table 1.

Table 1. UWA Kaolin clay properties.

Property	Value
Specific gravity, G_s*	2.6
Liquid Limit, LL (%)*	73.7
Plastic Limit, PL (%)*	44.4
Slope of normal consolidation line, λ*	0.435
Slope of swelling line, κ*	0.044
Coefficient of horizontal consolidation, c_h† (m²/year) at σ'_v = 70 kPa and OCR ~5.5	32

* Reid et al. (2024)
† Assessed from piezocone dissipation test

A T-bar penetrometer (Stewart & Randolph, 1994), with a diameter of 5 mm (D_T) and a length of 20 mm, was used to assess the undrained shear strength of the sample. The penetration rate of the T-bar (v_T) was set as 3 mm/s, resulting in a non-dimensional velocity ($V = v_T D_T / c_h$) equal to ~ 15, sufficient to ensure undrained conditions (Lehane et al., 2009). The horizontal coefficient of consolidation (c_h) was inferred from piezocone dissipation tests conducted with a 10 mm diameter piezocone that measures pore pressure at the u_2 (cone shoulder) position and analysed using the Teh & Houlsby (1991) solution. Four T-bar tests were conducted in the sample, which indicated an undrained shear strength of 34 kPa at the helix embedment depth. This value was derived from the measured T-bar penetration using a bearing capacity factor of 10.5 (Martin & Randolph, 2006).

2.2 Model helical anchor

The HEPLA model consists of a 25 mm diameter (D_{helix}) stainless steel helical plate with an 8 mm pitch, connected to an 8 mm diameter detachable follower shaft, thus modelling a 2 m diameter helix and 0.64 m diameter shaft at the testing acceleration of 80*g*. The HEPLA was also equipped with a swivel ring featuring a fin measuring 9 mm × 6 mm × 2 mm (height × width × thickness) to prevent the mooring from twisting around the shaft during installation, as shown in Figure 2. The mooring was modelled using a 1.3 mm diameter Dyneema rope with an ultimate tensile capacity of 1.2 kN. This was connected to the helix through a pair of holes at the top of the fin. The other end of the rope was connected to a 1 kN load cell mounted to an actuator.

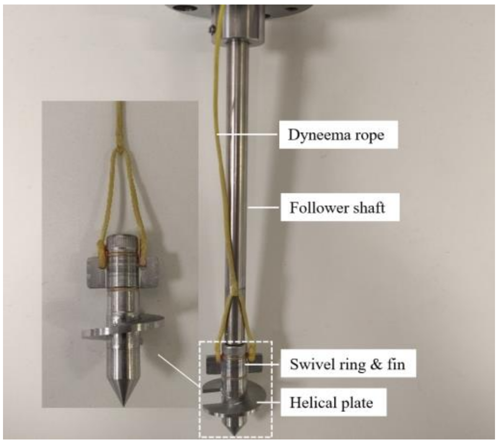

Figure 2. Reduced scale HEPLA model.

This paper considers three tests from a broader experimental program. These three tests are summarised in Table 2, and include two HEPLA tests (vertical and inclined loading) and one conventional helical anchor test with vertical loading. The latter was included to provide a basis for comparing the installation torque and capacity mobilisation for a HEPLA relative to an equivalent helical anchor, and as such, adopted a model helical anchor with a similar helix geometry and dimensions but with a slightly larger 10 mm diameter shaft.

Table 2. Experiments.

Test ID	Anchor type	Load direction
HP-VER	HEPLA	Vertical
HP-INC	HEPLA	Inclined
HX-VER	Standard helical anchor	Vertical

2.3 Experimental setup and procedure

The experimental arrangement is shown in Figure 3, with further details on the procedure illustrated in Figure 4a for vertical pull-out tests, and in Figure 4b for inclined pull-out tests. All HEPLA installations were initiated at 1*g* until the fin was just embedded in the soil (to hold the fin orientation and maintain the helix position during the remainder of the installation). The centrifuge was then spun to 80*g*, and sufficient time was allowed for pore pressure equalisation, as indicated by pore water pressure measurements made at the mid-height of the soil sample. All of the subsequent processes, including installation, shaft retrieval, and loading of the helical plate, were conducted inflight without stopping the centrifuge.

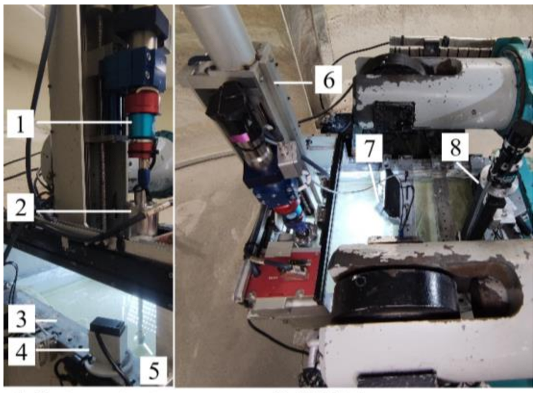

1. Rotary actuator
2. Torque & axial load cell
3. Strongbox
4. Surface camera
5. HEPLA
6. Primary 2D linear actuator
7. Underwater camera
8. Secondary linear actuator

Figure 3. Experimental arrangement in the beam centrifuge.

The testing procedures for vertical and inclined pull-outs are summarised schematically in Figure 4 and are described as follows:

1. *Helical anchor installation.* The HEPLA was installed using a rotary actuator (Duverneuil, 2024) that was located on the vertical axis of an electro-mechanical 2D actuator that allows motion along the vertical and horizontal directions. Axial force and torque during installation were measured by a load cell at the base of the rotary actuator. One end of the Dyneema rope was connected to the fin, while the other end was attached to a load cell, leaving some slack in the line during installation. The helical anchor was then installed at a vertical velocity of 2 mm/s. The rotation rate was set at 0.25 rev/s, resulting the *AR* equal to 1.
2. *Follower shaft retrieval*. As soon as the helix reached the target embedment depth, the follower shaft was retrieved by extracting it vertically at 1 mm/s and without rotation. A consolidation period of 3 hours (2.19 years in prototype scale) was allowed between shaft retrieval and the subsequent anchor loading.
3. *Anchor loading*. For vertical loading, the horizontal axis of the 2D actuator was displaced such that the vertical axis (and hence the load direction) was aligned with the centre of the helical plate (see step (3) in Figure 4a). The actuator was then moved upwards at a velocity

(v_e) of 1 mm/s, corresponding to a dimensionless velocity $V \sim 25$ ($V = v_e D_{helix}/c_h$, ensuring undrained loading), which tensioned the mooring line and mobilised the capacity of the anchor. For inclined loading, the mooring line was connected to a secondary linear actuator (labelled (8) in Figure 3) via a pulley located directly below this actuator (see step (3) in Figure 4b). Loading was also conducted at v_e = 1 mm/s ($V \sim 25$, such that anchor loading was also undrained) and was continued for 10 mm of line displacement after the peak anchor capacity was measured. The anchor was left in the sample and at the end of the testing the sample was dissected to reveal the anchor position and orientation.

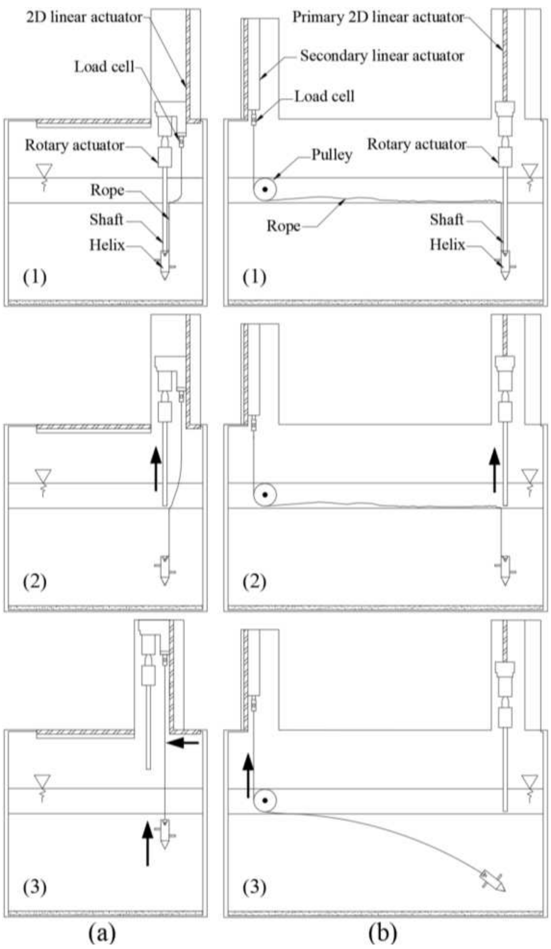

Figure 4. HEPLA centrifuge test procedure: (a) vertical loading; (b) inclined loading.

The standard helical anchor test adopted the same test procedures for installation and loading used for the HEPLA tests but without the pre-embedment at 1*g* and shaft extraction phases. A similar consolidation time was allowed between the end of installation and loading.

3 EXPERIMENTAL RESULTS AND DISCUSSION

3.1 Test programme summary

All experimental data, including installation torque (T), installation force (F), follower shaft retrieval force (R_F), and peak anchor capacity (Q_p), are presented in model scale unless specified otherwise. The maximum values, representing the key results, are provided in Table 3.

Table 3. Summary of HEPLA centrifuge test results.

Test ID	T (Nm)	F (N)	R_F (N)	Q_p (N)
HP-VER	0.23	90	19	218
HP-INC	0.23	91	21	247
HX-VER	0.32	111	-	229

3.2 Installation torque and force

The maximum installation torque measured in the two HEPLA tests was identical, at T = 0.23 Nm (118 kNm in prototype scale), whereas for the helical anchor installation, the maximum installation torque was 39% higher, T = 0.32 Nm (164 kNm in prototype scale). This difference is considered to be due to the larger (10 mm) diameter shaft used in the helical anchor test compared to the 8 mm diameter shaft used for the HEPLA tests. The maximum thrust force during installation was essentially identical for both HEPLA tests (F = 90 N and 91 N; 576 kN and 582 kN in prototype scale), whereas the maximum thrust force measured in the helical anchor installation was 23% higher at F = 111 N (710 kN in prototype scale).

3.3 Follower shaft retrieval force

The follower shaft retrieval force is due to the friction that develops at the shaft/clay interface as the follower is extracted. Measured shaft retrieval forces were adjusted to account for the submerged weight of the 120 mm long shaft, which resulted in R_F = 19 N and 21 N (122 kN and 134 kN in prototype scale).

3.4 Anchor capacity

Figure 5 shows the load-displacement response for the HEPLA under vertical (Figure 5a) and inclined (Figure 5b) loading. The displacement in Figure 5 corresponds to that of the actuator (measured using the encoder on the vertical axis motor), such that it does not account for the elongation of the Dyneema rope or other compliance in the system. Figure 5a also shows the net anchor capacity ($Q_{p,net}$) calculated as the peak measured load minus the submerged weight of the helical plate in clay. Additionally,

Figure 5a includes the capacity mobilisation response for the helical anchor test. In this case, the peak measured load is approximately equal to $Q_{p,net}$ as the load cell was zeroed before installation and pull-out (i.e., removing the anchor weight and buoyancy force). $Q_{p,net}$ for the HEPLA under vertical loading was 197 N, which is 14% lower than the 229 N measured in the helical anchor test. This difference may be attributed to the shaft resistance that develops in the case of a helical anchor but that is not present for the HEPLA. Adding the average 20 N shaft retrieval force would reduce this difference to 5%, noting that this would be reduced further if the shaft diameter used to install the HEPLA was the same as that on the helical anchor. Although Figure 5a indicates a much lower loading stiffness for the HEPLA, this is considered to be due (at least in part) to the stretch of the mooring.

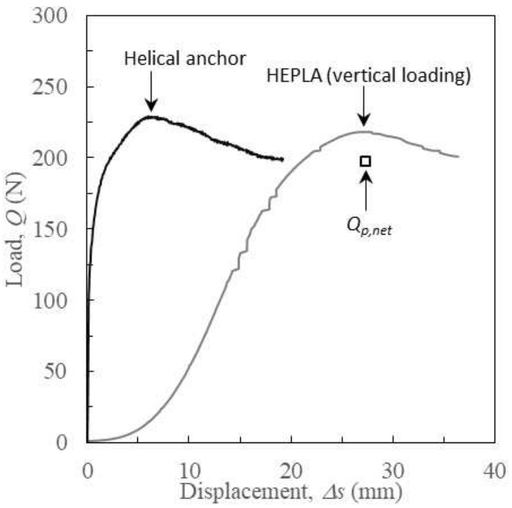

(a)

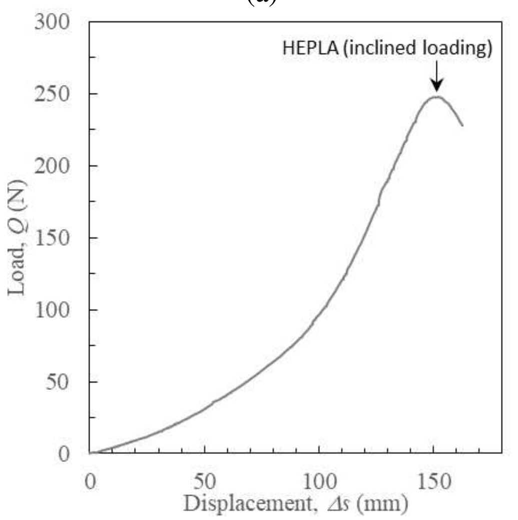

(b)

Figure 5. Capacity mobilisation response:(a) vertical loading (HEPLA and helical anchor); (b) inclined loading (HEPLA).

For the HEPLA under inclined loading, the measured capacity was Q_p = 247 N. This value is not corrected for the submerged weight of the helix and includes the contribution from the embedded mooring, which represents one of the main advantages of the HEPLA relative to a conventional helical anchor for inclined loads. As noted earlier in the paper, loading in the inclined HEPLA test was continued for an additional 10 mm beyond the point where the peak anchor capacity was observed. The test was then stopped, and the anchor was left in the soil until the end of the testing. Figure 6 shows the post-test anchor configuration, which clearly indicates that some degree of rotation occurred as the anchor aligned itself to the loading direction, maximising its projected area. The figure also shows that the line forms an inverse catenary profile, typical of embedded mooring chains (Neubecker & Randolph, 1995).

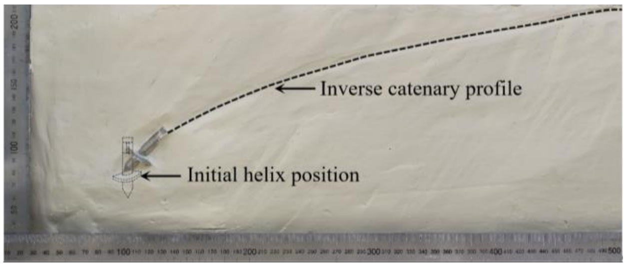

Figure 6. HEPLA position and orientation under an inclined load (just after the peak capacity).

4 CONCLUSIONS

This paper presents a series of proof-of-concept experiments conducted in a geotechnical centrifuge, that investigate the potential of a new helically embedded plate anchor (HEPLA). Tests were performed in overconsolidated kaolin clay, and the concept worked remarkably well in both vertical and inclined pull-out tests – with successful screw-in installations, shaft detachment/retrievals, and subsequent helical plate extractions.

The maximum torque required to install the HEPLA was 28% lower than for a ‘standard’ helical anchor. This difference may be attributed to the smaller shaft diameter used with the HEPLA, which could be even further optimised for field applications – as it only needs to be designed to meet structural requirements during installation.

Measured HEPLA capacities were similar to that measured in a reference helical anchor test, with small differences attributed to frictional resistance that develops along the shaft of a helical anchor and a capacity contribution of the embedded mooring. In addition to the advantages associated with reusing the installation follower, unlike a conventional helical anchor, the HEPLA is particularly suited to inclined loading as the embedded helical plate reorientates to the direction of loading – as confirmed from dissection of the sample after testing.

In summary, the testing reported here provides support to the potential of HEPLAs for floating offshore wind applications. The next step will be to assess its performance in other seabed types.

AUTHOR CONTRIBUTION STATEMENT

First Author: Conceptualization, Methodology, Validation, Investigation, Data curation, Formal Analysis, Writing - Original draft.
Second to Fifth Authors: Supervision, Writing - Reviewing and Editing, Technical discussions.
Sixth to Ninth Authors: Writing - Reviewing and Editing, Technical discussions.

ACKNOWLEDGEMENTS

The authors gratefully acknowledge financial support provided by the Australian Research Council, the University of Western Australia, and the Shell Chair in Offshore Engineering at The University of Western Australia. This work forms part of a larger collaborative project on helical anchors, conducted in partnership with Geowynd and the University of Dundee, whose support is also sincerely appreciated. The first author is grateful for the financial support from the Centre for Higher Education Funding (BPPT) and Indonesia Endowment Fund for Education Agency (LPDP). The fourth author leads the Shell Chair in Offshore Engineering research team at the University of Western Australia, which is sponsored by Shell Australia.

REFERENCES

Al-Baghdadi, T. A., Brown, M. J., Knappett, J. A., & Ishikura, R. (2015). Modelling of Lateral Loaded Screw Piles with large helical plates in sand. Front. Offshore Geotech, 503–508.

Bailey, H., Senior, B., Simmons, D., Rusin, J., Picken, G., & Thompson, P. M. (2010). Assessing underwater noise levels during pile-driving at an offshore windfarm and its potential effects on marine mammals. Mar. Pollut. Bull, 60(6), 888–897. https://doi.org/10.1016/j.marpolbul.2010.01.003

Byrne, B. W., & Houlsby, G. T. (2015). Helical piles: An innovative foundation design option for offshore wind turbines. Philos. Trans. R. Soc, 373(2035), 20140081. https://doi.org/10.1098/rsta.2014.0081

Cerfontaine, B., Brown, M. J., Knappett, J. A., Davidson, C., Sharif, Y. U., Huisman, M., Ottolini, M., & Ball, J. D. (2023). Control of screw pile installation to optimise performance for offshore energy applications. Geotechnique, 73(3), 234–249. https://doi.org/https://doi.org/10.1680/jgeot.21.00118

Davidson, C., Brown, M. J., Cerfontaine, B., Al-Baghdadi, T., Knappett, J., Brennan, A., Augarde, C., Coombs, W., Wang, L., Blake, A., Richards, D., & Ball, J. D. (2022). Physical modelling to demonstrate the feasibility of screw piles for offshore jacket-supported wind energy structures. Géotechnique, 72(2), 108–126. https://doi.org/10.1680/jgeot.18.P.311

Dove, P., Treu, H., & Wilde, B. (1998, November). Suction embedded plate anchor (SEPLA): a new anchoring solution for ultra-deepwater mooring. Proc. Deep Offshore Tech. Conf.

Duverneuil, P. Y. G. (2024). The response of helical anchors under offshore environmental loading. PhD thesis, University of Western Australia.

Lehane, B. M., O'Loughlin, C. D., Gaudin, C., & Randolph, M. F. (2009). Rate effects on penetrometer resistance in kaolin. Géotechnique, 59(1), 41–52. https://doi.org/https://doi.org/10.1680/geot.2007.00072.

Martin, C. M. & Randolph, M. (2006). Upper-bound analysis of lateral pile capacity in cohesive soil. Géotechnique 56(2), 141–145. https://doi.org/10.1680/geot.2006.56.2.141.

Neubecker, S. R., & Randolph, M. F. (1995). Profile and Frictional Capacity of Embedded Anchor Chains. J. Geotech. Eng, 121(11), 797–803. https://doi.org/10.1061/(ASCE)0733-9410(1995)121:11(797)

O'Loughlin, C. D., Blake, A. P., Wang, D., Gaudin, C., & Randolph, M. F. (2013). The dynamically embedded plate anchor: Results from an experimental and numerical study. Proc. Int. Conf. Offshore Mech. Arctic Eng. - OMAE, 6. https://doi.org/10.1115/OMAE2013-11571

Reid, D., Fanni, R. & Fourie, A. (2024). A SHANSHEP approach to quantifying the behaviour of clayey soils on a constant shear drained stress path. Can. Geotech. J., 61, 1517–1540. http://dx.doi.org/10.1139/cgj-2022-0473

Stewart, D. P., & Randolph, M. F. (1994). T-Bar Penetration Testing in Soft Clay. J. Geotech. Eng, 120(12), 2230–2235. https://doi.org/10.1061/(ASCE)0733-9410(1994)120:12(2230)

Teh, C. I., & Houlsby, G. T. (1991). An analytical study of the cone penetration test in clay. Géotechnique, 41(1), 17–34. https://doi.org/10.1680/geot.1991.41.1.17

Ullah, S. N., O'Loughlin, C., Hu, Y., & Hou, L. F. (2024). Torsional installation and vertical tensile capacity of helical piles in clay. Géotechnique, 74(12), 1360–1376. https://doi.org/10.1680/jgeot.22.00014